Trends in
Applied Sciences Research

Academic Journals Inc.

The Applying of THz and Raman Techniques
in Non-destructive Examination for Nitrobenzoic Acid

Luo Zhixun, Fang Yan and Zhao Guozhong
Beijing Key Lab for Nano-photonics and Nano-structure, Department of Physics,
Capital Normal University, Beijing 100037, People's Republic of China

Abstract: The strong absorption spectrum of Nitrobenzoic acid at THz wave band was obtained. Applying the THz and Raman techniques we studied the lowest vibrational modes of Nitrobenzoic acid, which could be used to determine its isomeric conformation. This method has important applications in identifying specific molecules based on their vibrational properties. It also shows that the analysis of time-domained spectrum in the far infrared, coincided with Raman spectrum techniques, may be a non-destructive and very direct way of obtaining information about the shape of the molecular skeleton during and after photo excitation.

Key words: THz, Raman, Nitrobenzoic acid, non-destructive, vibrational, rotational

Introduction

In the frame of molecular energy level, the vibrational and even rotational energy levels are usually represented by the infrared and Raman spectroscopy. Actually for each molecule, the infrared and Raman spectroscopy have almost formed a series of dactylogram. However, they still cannot always reflect all the energy information of molecular fine structure. Just as some Raman active modes representing non-active in infrared region and some infrared active modes vanished in Raman spectra, the rotational energy levels based on some vibrational energy level varied with the quantum number J increasing may not detected by infrared and Raman spectroscopy (Shimizu *et al.*, 1994; Giner *et al.*, 1996; Goodman, 1996).

Earlier studies by Jackson (1975), Durchschlag (1981). Tempel and Gondar (1986) of the infrared properties of adenosine and cytidine concentrated on the frequency region above 200 cm^{-1}, due to lack of theoretical results for external modes below the frequencies. The origin of the lowest-frequency Raman mode in guanosine and nucleotides. The Raman spectrum of self-associated guanosine and interpreted modes below 100 cm^{-1}as associated with hydrogen bonding between the molecules. Because the global shape of the multi-dimensional potential energy function of the molecules determines the properties of low-frequency vibrational modes in large molecules. Therefore, the frequencies of the lowest normal modes of a molecule can be highly sensitive to the geometric arrangement of atoms within the molecule. The terahertz (THz) probe pulses consist of a single cycle of the electromagnetic field with a duration of less than 1 ps, covering the spectral range 0.1-2.7 THz (0.4-11 meV), exhibiting properties for both sides of the electromagnetic spectra (Pickett *et al.*, 1984; Winnewisser *et al.*, 1997; You and Bucksmand, 1997; Bromage *et al.*, 1997; Darrow *et al.*, 1992).

Corresponding Author: Fang Yan, Beijing Key Lab for Nano-photonics and Nano-structure, Department of Physics, Capital Normal University, Beijing 100037, People's Republic of China

As we know, both THz wave and Raman techniques are suitable for chemical component detection purposes, no damage to samples, being able to screen the measurement results having proven the existence of fingerprint spectra in the corresponding region. Owing to the wide range frequency band of THz pulse and Raman, much information besides what Infrared can represented may be detected. It means wide application foreground, as well as a new technique field of interdisciplinary collaborating investigation. However, because of the different mechanism of THz with Raman spectra, once an organic relationship between them for all kinds of molecules is set up, more comprehensive information may be obtained such as molecular structure and movement, including its vibrational and rotational energy levels (Markus Walther *et al.*, 2000; Durchschlag and Temple, 1981; Nuss *et al.*, 1987).

In this study, the strong absorption spectra of Nitrobenzoic acid at THz wave band were obtained. It demonstrated that the lowest vibrational modes of Nitrobenzoic acid could be used to determine its isomeric conformation. This information has important applications e.g., recognition of specific molecules based on their vibrational properties; it also shows that time-resolved vibrational analysis in the far infrared, coinciding with Raman spectrum techniques, may be a very direct way of obtaining information about the shape of the molecular skeleton during and after photo excitation.

Materials and Methods

Sample Preparation

The samples, in the form of powders, were carefully mixed with Polyethylene (PE) powder with varying weight ratios about 1:2, depending on the absorption strength of the sample material and pressed into 1mm thick pellets. PE has low absorption ($<5\ cm^{-1}$ below 4 THz) and constant index of refraction in the range between 0.1 and 4 THz), slightly depending on the pressure applied during sample preparation.

Thz and Raman Instruments

We use a THz time-domain spectrometer setup with an optical layout was used in this experiment. The photoconductive antennas are driven by pulses of 30 fs duration from a Ti:sapphire oscillator. One of the antennas is used as a THz pulse emitter and the other one as a field-sensitive THz detector, gated by a second portion of the fs beam. The emitter consists of 10 μm wide metallic electrodes lithographically deposited on a semi-insulating InAs wafer. Charge carriers excited to the conduction band of the InAs substrate by the laser pulse are accelerated by the strong bias field, thereby emitting a short burst of electromagnetic radiation. The power of fs laser pulse used in our experiment is 400 mW and the available frequency range is 0.2-2.5 THz. Detect method adopt the electrical optical sampling technique with the ZnTe wafer as field-sensitive detector (<110> ZnTe). The Reference pulse and sample pulse spectra are all obtained in nitrogen environment withthe environment temperature at 23°C and relative humidity at 39% (Marcuvitz, 1951; Uhd Jepsen and Keiding,1996).

Raman spectra are recorded by an RFS 100/s FT-IR spectrophotometer (excited at 1064 nm). The exciting laser power is 50 mW for all samples.

Data Analysis Method for THz

The electric field of a THz pulse transmitted through a sample is modified by dispersion and absorption of the sample. The two fields recorded in the experiment are the reference field Er (t)

(THz electric field propagating through the empty reference aperture) and the sample field Es (t) (THz electric field propagating through the sample). Subsequent to recording, these fields are Fourier transformed to yield Es(v) and Er(v). The ratio of the complex fields is Es(v)/Er(v) = T (n) exp{.α(v)d + in(v)2πvd/c} (1) where, d is the thickness of the sample, v = ω/2π is the frequency of the radiation, c is the speed of light in vacuum and T (n) is a factor which accounts for reflection losses at the sample surfaces. In this way, both the refractive index n and the absorption coefficient of the sample α can be determined from the ratio of the measured THz fields. The molar absorption coefficient is obtained from α and the concentration K of the sample material (Uhd Jepsen and Keiding, 1995; Takeuchi *et al.*, 1997).

Results and Discussion

Figure1a shows THz pulses before and after propagation through a sample of 2-Nitrobenzoic pill (left) in nitrogen environment at temperatures about 295 K and the right one shows another pulses before and after propagation through a sample of for 4-Nitrobenzoic pill (right). As we can see, there is both obvious delay time between reference pulse and sample pulse; besides, the signals of reference pulses are always stronger than sample pulses. In fact, the signals of two samples are different. It is due to the sample's refractive index that is bigger than that of nitrogen itself. And it suggests that different sample shows different absorption to THz wave.

Figure 2a and b present the FFT spectra corresponding to the relationship of swing and frequency and Fig. 2c refers to the Absorption band of 2-Nitrobenzoic at temperatures about 295 K. As we can see, there is a big absorption band at the whole. In addition, a number of peaks in the spectrum are presented, especially in the higher frequency region, such as 1.67 and 2.2 THz, which turn out to be extremely sharp and strong. In addition, there are four weak peaks shown in the lower frequency region.

Similarly, Fig. 3a and b aim at the Corresponding intensity spectra (upper); and Absorption band of 4-Nitrobenzoic at temperatures about 295 K (below). As we can see, the structures of 2-Nitrobenzoic and 4-Nitrobenzoic molecules have the only difference of the site of the nitro-group. However, they almost show no same absorption modes in lower frequency. On the contrary, the sharpest and strongest peak in the cure is presented at 1.2 THz. And another three peaks appeared in the higher frequency region, as shown at 1.84, 2.04 and 2.2 THz, which turns out to be a big wave packet at the whole. And it even presents a shoulder absorption peak for 1.84 Thz band. Including the corresponding absorption band, these different absorption peaks may provide proofs that these absorption modes in THz wave band result from the different transition between rotational energy intervals based on some vibration energy.

Besides the THz spectrum presents the great difference between the two molecules, the Raman spectra, as shown in Fig. 4, clearly reflected the comparability and difference. Where Fig. 4a shows the Raman of polythene pill in order to exclude the interference Raman peaks and Fig. 4b and c refer to Raman spectra of the same pills of 4-Nitrobenzoic and 2-Nitrobenzoic that used in THz experiments and intermingled with polythene.

The strongest peak in the two spectra at 1363 cm^{-1} almost appeared at the same frequency, which assigned to $-NO_2$ symmetric stretching. And the mode of C-C stretching of benzene at 1598 cm^{-1} (1607 cm^{-1}), including the shoulder peaks at 1639 cm^{-1} (1638 cm^{-1}), also presents the reasonable similarity. In addition, the mode of COO-bending appeared at 861 cm^{-1} (860 cm^{-1}) also plays no difference between the two spectra. However, there is still some difference remarkable, for

example, there is some red shift of all the modes in the lower frequency for Fig. 1c compared to Fig. 1b, such as the band at 265 cm^{-1} (274 cm^{-1}), 522 cm^{-1} (532 cm^{-1}), 628 cm^{-1} (642 cm^{-1}). And the band at 3081 cm^{-1} also presents another dramatic phenomenon, where the two sharp brother peaks in Fig. 4c turn blunt even look like a narrow wave packet. These differences in Raman spectra reflect the structure of the two molecules. With these fingerprint spectra, we also can easily identify this kind of molecules from each other.

The spectrum of each molecule is dominated by a series of resonances distributed between 1 and 3.5 THz. Each resonance is observed as an absorption peak with a corresponding characteristic change of the index of refraction. These modes may refer to the vibrational and rotational energy level of molecules.

Considering the total energy of molecular inside as $E = E_e + E_v + E_r$, where, E_e is for the energy of electron movement, while E_v and E_r refer to vibrational and rotational energy of molecules. Since every kind of movement energy is quantized, when the molecular phase jumps from E'' to $E'(<E'')$, it will emit electromagnetic radiation of which frequency is determined by:

$$v = \frac{E'' - E'}{h} = \frac{1}{h}[(E''_e + E''_v + E''_r) - (E'_e + E'_v + E'_v)] = \frac{\Delta E_e}{h} + \frac{\Delta E_v}{h} + \frac{\Delta E_r}{h} = v_e + v_v + v_r \qquad (1)$$

Proved by theories and experiments, the energy difference of electron movement ΔE_e is the largest, while v_e is the smallest and even usually $v_e > v_v < v_r$. This means there may be vibrational energy levels at every electron energy level, while rotational energy levels with smaller energy differences based on the vibrational energy level as well.

According to Formula (1), the molecular spectra seem are composed of some discrete lines. However, it is not difficult to image, when the electron transition occur from one orbit to another, it will lead to the emission or absorption of radiation, as well as the changes of molecular electron cloud distribution and the internuclear electrostatic forces. This may result in influence to the molecular binding force and internuclear distance, which force the molecule to establish a new balance. So the molecular electron transition, changes of E_e, must lead to the changes of interatomic vibrational phase, shown in changes of E_e. Similarly, the vibrational phase changes may bring the increasing or decreasing of general molecular moment of inertia. So do the rotational phase changes. In brief, the molecular transition must bring along the transition between vibrational and rotational energy levels.

Because the energy difference ΔE_e is usually about 1-20 eV, the electron spectra result from transitions among electron energy levels, besides a few in near-infrared region, mainly locate in UV or visual field. While the transition between vibrational energy level or rotational energy level may be in infrared or far-infrared region.

On the one hand, if the electron energy and vibrational energy, except the rotational energy, of molecules show no changes ($\Delta E_e = \Delta E_v = 0$; $\Delta E_e \neq 0$), then: $v = \Delta E_r / h = v_r$ which presents the pure rotational spectra. Regarding to the rotational energy interval ΔE_r is usually less than 0.05 eV, even below 10^{-4}, so the pure rotational spectra usually lies in the far-infrared or microwave region about 25-1000 μm. As we know, the metal bond vibration of some metallorganics, including many bond vibrations and even crystal lattice vibrations of crystal, may also occur far-infrared spectra.

On the another hand, if the vibrational and rotational energy levels both changed but the electron energy, ($\Delta E_e = \Delta E_v = 0$; $\Delta E_e \neq 0$), then the radiation frequency:

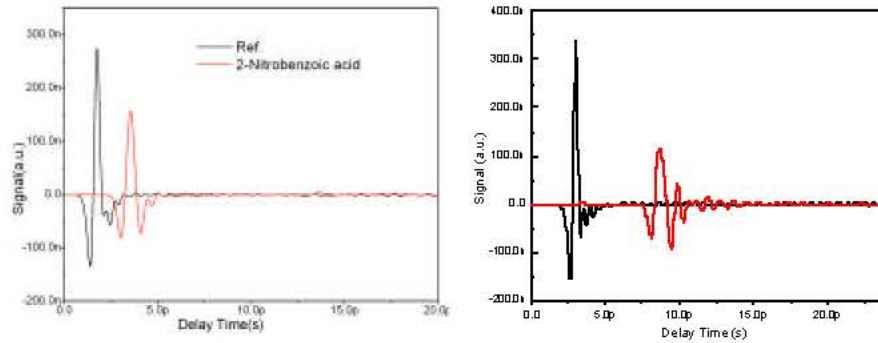$$v = \frac{\Delta E_v + \Delta E_r}{h} = v_v + v_r \qquad (2)$$

Fig. 1: THz pulses before and after propagation through a sample of 2-Nitrobenzoic pill (left); and 4-Nitrobenzoic pill (right)
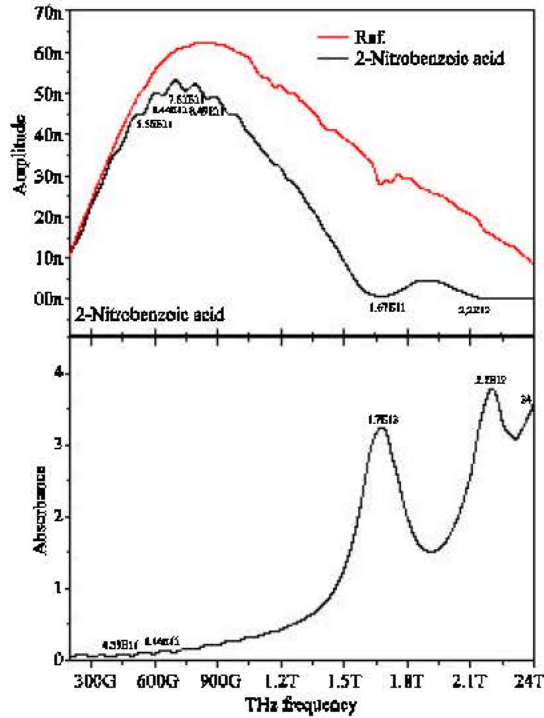

Fig. 2: Corresponding intensity spectra. (upper) and Absorption band of 2-Nitrobenzoic at temperatures about 295 K (under)
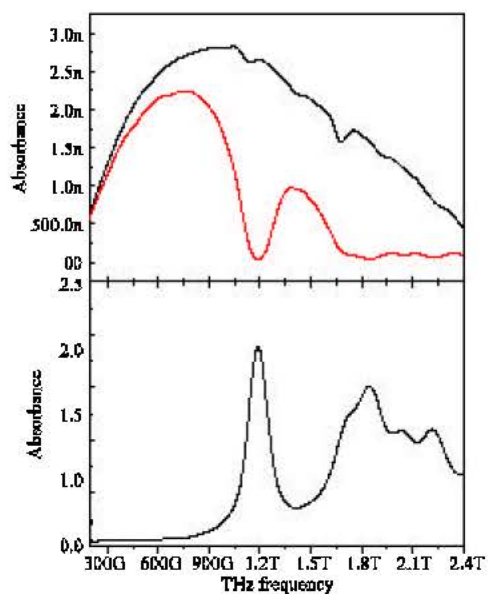
Fig. 3: Corresponding intensity spectra. (upper) and Absorption band of 4-Nitrobenzoic at temperatures about 295 K (under)
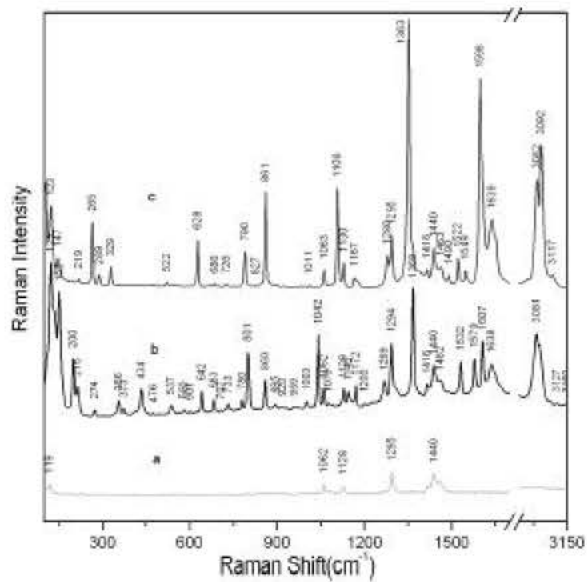

Fig. 4: Raman spectroscopy Raman of polythene pill (a) and that of 4-nitrobenzoic (b); 2-Nitrobenzoic (c) pill intermingled with polythene

Here, it means the molecular vibration-rotational spectra. Owing to the vibrational energy difference is usually 0.05-1eV, the basic frequency vibration-rotation spectra aim at 2.5-25 μm as known as middle-infrared region, but the extensive frequency band of molecular vibration, as well as combination frequency band, refers to near-infrared region of 0.75-2.5 μm. Since the vibrational phase changes cannot but bringing the varying of general molecular moment of inertia and rotational energy, it is obvious that the pure vibrational spectra couldn't be observed.

Conclusions

The strong absorption spectrum of Nitrobenzoic acid at THz wave band was obtained. And we demonstrated that the lowest vibrational modes of Nitrobenzoic acid could be used to determine its isomeric conformation. This information has important applications in, e.g., recognition of specific molecules based on their vibrational properties; it also shows that time-resolved vibrational analysis in the far infrared, coinciding with Raman spectrum techniques, may be a very direct way of obtaining information about the shape of the molecular skeleton during and after photo excitation. Due to their collective nature such modes are highly sensitive to the intra- and intermolecular structure and thus provide a unique fingerprint of the conformational state of the molecule and effects of its environment.

Acknowledgements

References

Bromage, J., S. Radic, G.P. Agrewal, C.R. Jr. Stroud, P.M. Fauchet and R. Obolewski, 1997. Spatiotemporal shaping of terahertz pulses. Opt. Lett., 22: 627.

Darrow, J.T., X.C. Zhang, D.H. Auston and J.D. Morse, 1992. Saturation properties of large-aperture photoconducting antennas. IEEE J. Quantum Electron, 28: 1607.

Durchschlag, M.S. and T.A. Temple, 1981. Far-IR optical properties of freestanding and dielectrically backed metal meshes. Applied Opt., 20: 1245.

Giner, C. and J. Gondar, 1986. Exact wave functions and energy levels for a quantum well with an applied electric field. Physica, B 138: 287.

Goodman, J.W., 1996. Introduction to Fourier Optics. 2nd Edn., McGraw-Hill, New York.

Jackson, J.D., 1975. Classical Electrodynamics. 2nd Edn., John Wiely and Sons, New York.

Marcuvitz, N., 1951. Waveguide Handbook. McGraw-Hill Book Company, New York.

Markus, W., K. Jensby and S. Rud Keiding, 2000. Far-infrared properties of DAST; June 15, 2000 / Vol. 25, No. 12 / OPTICS LETTERS

Nuss, M.C., D.H. Auston and F. Capasso, 1987. Direct subpicosecond measurement of carrier mobility of photoexcited electrons in gallium arsenide. Phys. Rev. Lett., 58: 2355.

Pickett, H.M., J. Farhoomand and A.E. Chiou, 1984. Performance of metal meshes as a function of incidence angle. Applied Opt., 23: 4228.

Shimizu, A. and M. Yamanishi, 1994. Photon-energy dissipation caused by an external electric circuit in "virtual" photoexcitation processes. Phys. Rev. Lett., 72: 3343.

Takeuchi, T., S. Sota, M. Katsuragawa, M. Komori, H. Takeuchi, H. Amano and I. Akasaki, 1997. Quantum-confined Stark effect due to piezoelectric fields in GaInN strained quantum wells. Jpn. J. Applied Phys. Part 2 36, L382.

Uhd Jepsen, P. and S.R. Keiding, 1995. Radiation patterns from lens-coupled terahertz antennas. Opt. Lett., 20: 807.

Uhd Jepsen, P., R.H. Jacobsen and S.R. Keiding, 1996. Generation and detection of terahertz pulses from biased semiconductor antennas. J. Opt. Soc. Am. B., 13: 2424.

Winnewisser, C., P. Uhd Jepsen, M. Schall, V. Schyja and H. Helm, 1997. Electro-optic detection of THz radiation in LiTaO3, LiNbO3 and ZnTe. Applied Phys. Lett., 70: 3069.

You, D. and P.H. Bucksbaum, 1997. Propagation of half-cycle far infrared pulses. J. opt. Soc. Am. B., 14: 1651.